

Laser Metrology Gauges for OS1

Yekta Gürsel

Jet Propulsion Laboratory
California Institute of Technology
4800 Oak Grove Dr., Pasadena, CA 91109

ABSTRACT

Heterodyne interferometers have been commercially available for many years. In addition, many versions have been built at JPL for various projects. This activity is aimed at improving the accuracy of such interferometers from the 1-30 nanometer level to the picometer level for use in the proposed OS1 and SONATA missions as metrology gauges. In the null-gauge configuration, we obtained a precision of 0.6 picometers at time scales of 2,500 seconds. In the relative-gauge configuration, we obtained an accuracy of 3.5 picometers rms in vacuum at time scales of few minutes. An absolute gauge with an accuracy of 10 microns over a distance of 10 meters is under construction.

1 INTRODUCTION

The Orbiting Stellar Interferometer (OSI) requires metrology interferometers with a relative accuracy of 1-2 root-mean-squared (rms) picometers to attain its design goals. In the current design, these interferometers are one-long-arm, heterodyne interferometers which monitor the distance between two corner cubes.

Three different implementations of the basic gauge architecture have been examined. The null-gauge experiment determines the ultimate precision of heterodyne interferometers by using two of these with spatially coincident beams. The relative-gauge experiment determines the extent of systematic errors which are absent in the null configuration by measuring small distances (few wavelengths of light) from a given set point. The absolute metrology gauge measures the distance between two points to an absolute accuracy of 10 microns. The design of OSI allows the absolute metrology gauge to be much less accurate than the relative metrology gauges [1].

2 NULL METROLOGY GAUGE

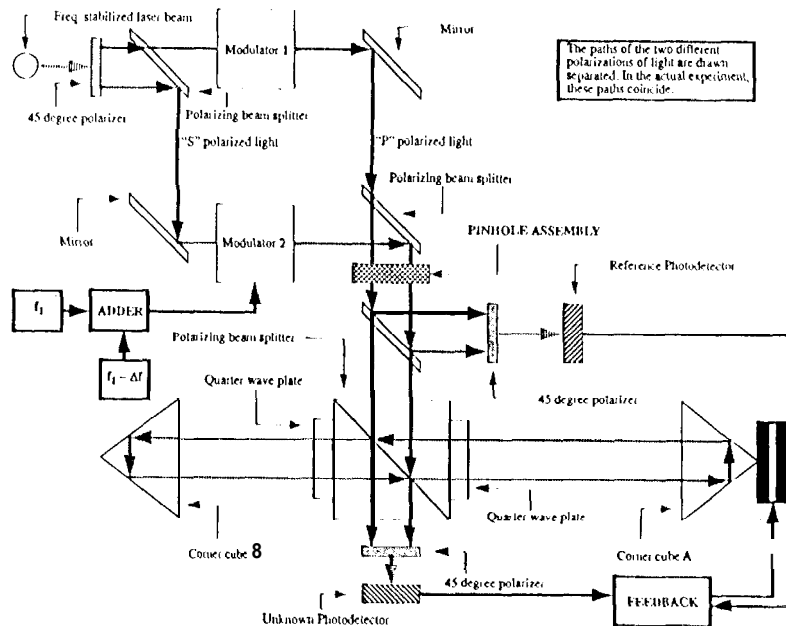
The null-metrology gauge consists of two heterodyne interferometers with spatially coincident light paths. As our vacuum chamber had not yet been delivered at the time this experiment was performed, we chose this scheme to eliminate the effect of the density fluctuations in air which limit the accuracy of the interferometers to ~10 nanometers rms. One of the interferometers is used to servo the distance being monitored to the null of the interferometer, while the other interferometer is used as a read-out device.

The schematic layout of the experiment is shown in Fig. 1. The light from a frequency-stabilized He-Ne laser impinges on a 45 degree linear polarizer. The light from the output of the polarizer is separated into two orthogonal polarizations (S and P) by a suitably placed polarizing beam splitter. Each of these polarizations is then routed through an acousto-optic modulator.

These modulators are driven by CB radios with a frequency difference of 10 kHz. The frequency shifted beams are then recombined by another polarizing beam splitter. The recombined beam is sent through a pin-hole assembly to spatially filter the beam. The spatial filtering also makes the output beam insensitive to the directional fluctuations of the input beam.

A small part of this beam is then diverted into a 45 degree polarizer and a photodiode which acts as a reference detector. The rest of the beam enters a beam-launcher assembly which consists of a polarizing beam splitter and two quarter-wave plates. Half of the beam directly passes through the polarizing beam splitter and strikes the photodetector after passing through a 45 degree polarizer. The other half of the beam makes a round trip between

Figure 1: The Null Metrology Gauge



the corner cubes and exits the interferometer coincident with the first half of the beam and hits the photodetector after passing through the same polarizer. The corner cubes are separated by a nominal distance of ~ 75 cm.

The relative phase of the signal coming out of the latter photodetector (the unknown photodetector) with respect to the phase of the signal coming out of the reference detector is directly a measure of the distance between the two corner cubes. In effect, the heterodyne interferometer converts an actual path-length change of one light wavelength into a phase change of one cycle of a sinusoidal wave at a frequency equal to the difference between the two driving frequencies of the acousto-optic modulators [2].

The set-up as described above consists of a single heterodyne interferometer. In order to place another interferometer which has very-nearly-the-same optical path, we added another driving signal to one of the modulators. The frequency of this driving signal is 20 kHz more than the frequency of the signal applied to the other modulator.

In this case, the outputs of the reference and the unknown photodetectors contain 3 signals at the frequencies of 10 kHz, 20 kHz and 30 kHz. The 10 kHz and the 20 kHz signals are separated from each other and the 30 kHz signal by an assembly of notch filters which also perform some 120 Hz rejection to enable us to work under normal lighting without saturating the amplifiers.

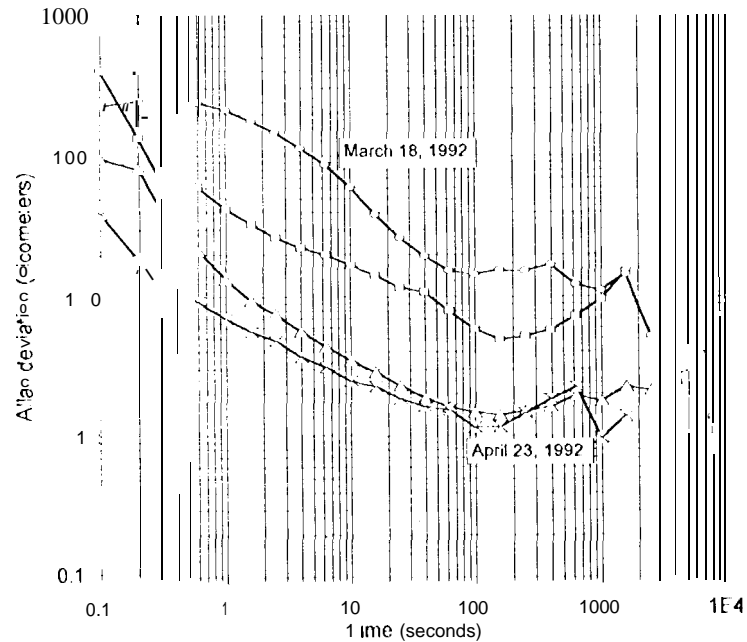
These sinusoidal signals are amplified and converted into square-wave signals by a post-amplifier circuit consisting of filters and comparators. The square-wave signals are then fed into a phase digitizer which digitizes the relative phase of the 10 kHz unknown, 20 kHz reference and the 20 kHz unknown signals with respect to the phase of the 10 kHz reference signal.

The relative phase signal from the 10 kHz interferometer is digitally processed and converted back into an analog feedback signal which is applied to a piezo-electric transducer. This transducer translates one of the corner cubes to hold the 10 kHz interferometer at null.

The relative phase signals from both interferometers are digitally recorded on a magnetic disk during the experiment. The data are analyzed after the recording is completed.

The results of various runs between March 18, 1992 and April 23, 1992 are shown in Fig. 2. The Allan deviation (square root of Allan variance) of the difference between the 10 kHz and the 20 kHz interferometer signals is plotted as a function of the integration time. The curve which has the largest overall Allan deviation is plotted using our first data. The curve which has the lowest overall Allan deviation was plotted using data taken on April 23, 1992. The reason for the dramatic improvement was the elimination of scattered light reflected back towards the laser.

Figure 2: Null metrology results



The servo system had also been improved during that time which lowered the low-integration-time parts of the curve. The best result using this configuration was a difference deviation of 1.3 picometers at an integration time of 100 seconds. The curve then slowly rose to 2 picometers at integration times close to 4,000 seconds.

We determined the cause of the upward drift at long integration times to be the temperature sensitivity of the electronic circuits which amplify and shape the analog signals. As the data were being taken, the drifting room temperature caused the various components in the electronics circuits to drift. Since the 10 kHz and the 20 kHz interferometers used different sets of electronics, a time varying phase difference was introduced because of the small differences between the circuits due to component tolerances.

To reduce the effect of this temperature related slow drift, we constructed a switching network which swapped the entire sets of amplifier and shaping circuits between the interferometers at regular intervals (30 sec). The circuits were also upgraded using low temperature coefficient, precision components.

The results of these modifications is shown in Fig. 3. As a reference, the Allan deviation from the April 11, 1992 data is also shown. The new data give an Allan deviation for the difference signal between the interferometers which reaches down to 0.6 picometers at integration times of 2,500 seconds and it stays under 2 picometers at integration times of 10,000 seconds.

3 RELATIVE METROLOGY GAUGE

The relative metrology gauge consists of two heterodyne interferometers with spatially separated paths as shown in Fig. 4 and Fig. 5. Since the physical laser beams do not overlap, each acousto-optic modulator is driven with a single frequency. The frequency difference between the drives to the acousto-optic modulators is 10 kHz. One of the interferometers is used to servo the distance between the corner cubes to a slowly varying separation, while the other interferometer is used as a read-out device.

The relative metrology experiment is designed to classify and eliminate various sources of systematic errors which are absent in a null-metrology gauge. The polarization leakage caused by several imperfect optical elements (Fig. 6) causes a systematic error at the output of the interferometer which is a periodic function of the distance between the corner cubes with a period of exactly one wavelength. The amplitude of this systematic error could be as large as 10 nanometers.

Figure 3: Null metrology with electronic switching

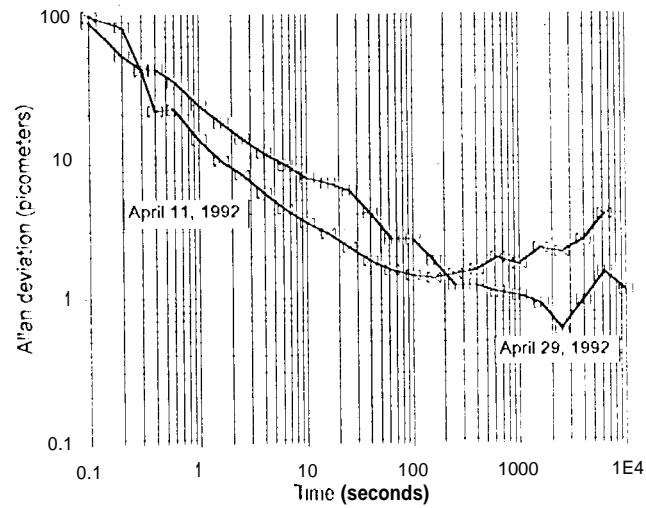


Figure 4: Relative metrology interferometer (a)

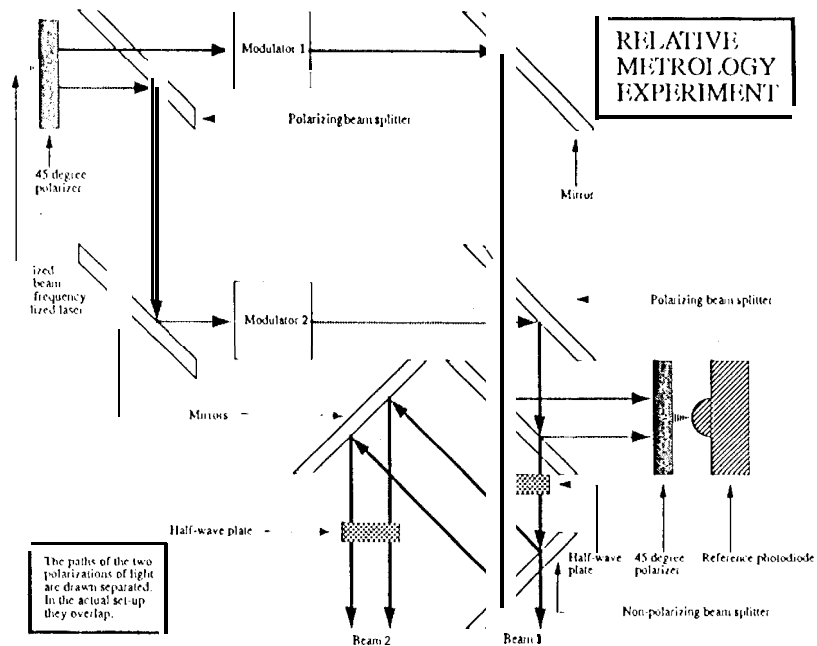


Figure 5: Relative metrology interferometer (b)

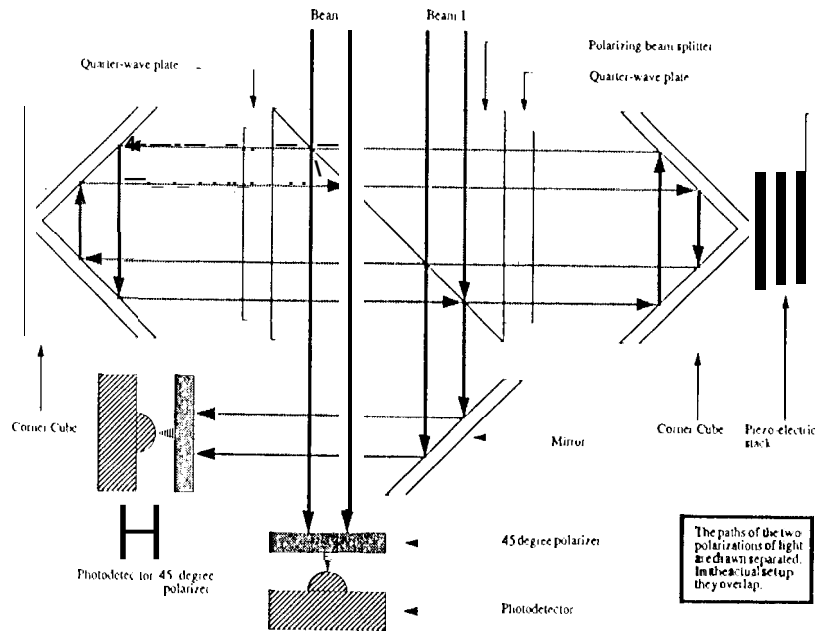


Figure 6: Polarization leakage (self-interference)

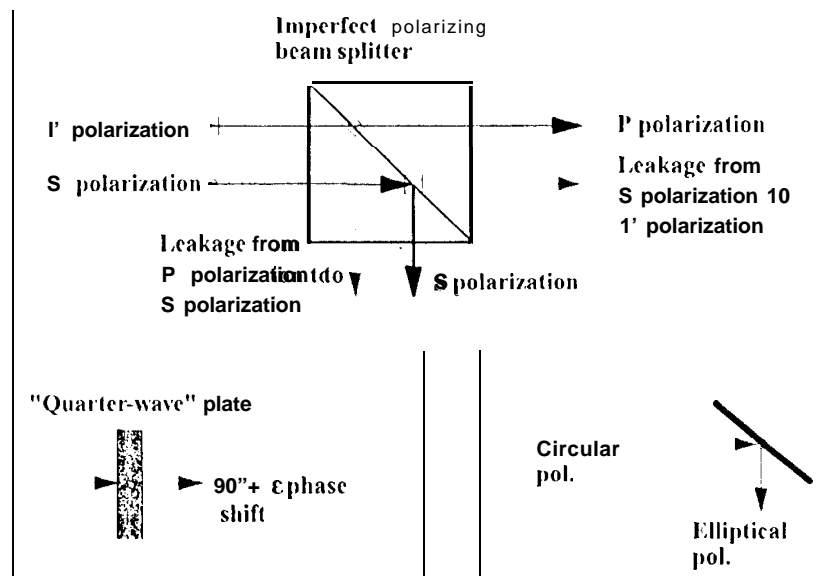
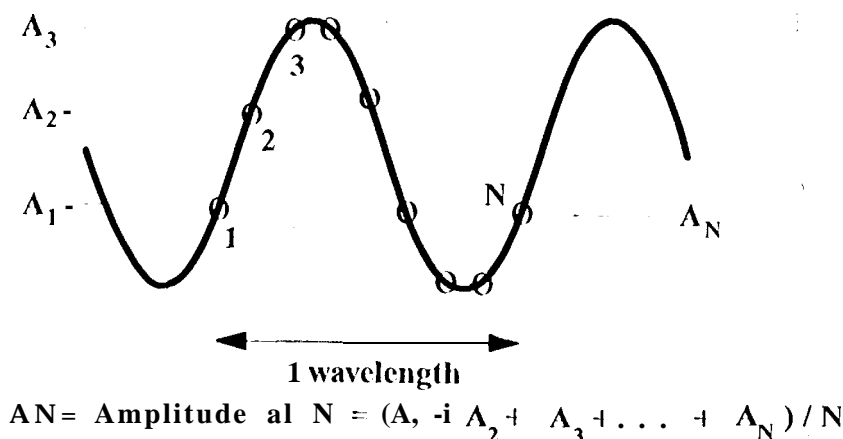


Figure 7: Cyclic averaging



These systematic errors can be classified into two categories: The periodic systematic errors due to the polarization leakage with a period of exactly one wavelength and the systematic errors caused by temperature gradients which appear as a small linear drift over short time scales between the readings of the interferometers. In this paper, we will consider only the periodic, systematic errors. The temperature gradient related errors are minimized by actively stabilizing the temperature of various optical components and by performing the relative measurements quickly before a significant drift accumulates.

The periodic systematic errors are eliminated by using a method known as cyclic averaging (Fig. 7). This is implemented by either modulating the distance to be measured with a piezoelectric transducer or by sweeping the laser frequency at a fast rate compared to the changes in the distance being measured. The amplitude of the modulation is chosen to be several wavelengths of light. The output of each interferometer is recorded at a rate to guarantee many readings during one wavelength of motion due to modulation. The true output of the interferometer at the center of modulation is computed to be the average over one exact wavelength of the modulated readings around the center of modulation.

In the actual experiment, a wavelength is divided in 64 equal parts. The servo is used to advance the distance by one sixty-fourth of a wave at a time while covering several wavelengths. At each step a few seconds of data is collected from the interferometers. The average value of each interferometer reading over this time interval is subtracted from each other. In the absence of any systematic errors, this difference is of the order of few picometers as determined by the null gauge. Since the laser beams travel through different parts of the optical components, the systematic errors which are present on the interferometer signals are different and do not cancel out when the readings of the two interferometers are subtracted.

Fig. 8 shows the result of cyclic averaging applied to the difference signal between the two interferometers. The data are taken in a closed vacuum chamber under atmospheric pressure. After the linear drift is taken out, the residual error is 31 picometers rms.

Fig. 9 shows the same experiment performed under vacuum after cyclic averaging. After the linear drift is taken out, the residual error is 10 picometers rms.

If the amplitude of the self-interference is changing due to various alignment drifts, cyclically averaging the data once will not remove all the systematic errors. In this case, the cyclic averaging can be used repeatedly until all systematic errors disappear. The actual gauge signal can be recovered after these integrations provided that the true signal is varying slowly compared to the total integration time.

Figure 8: Relative metrology with cyclic averaging in air

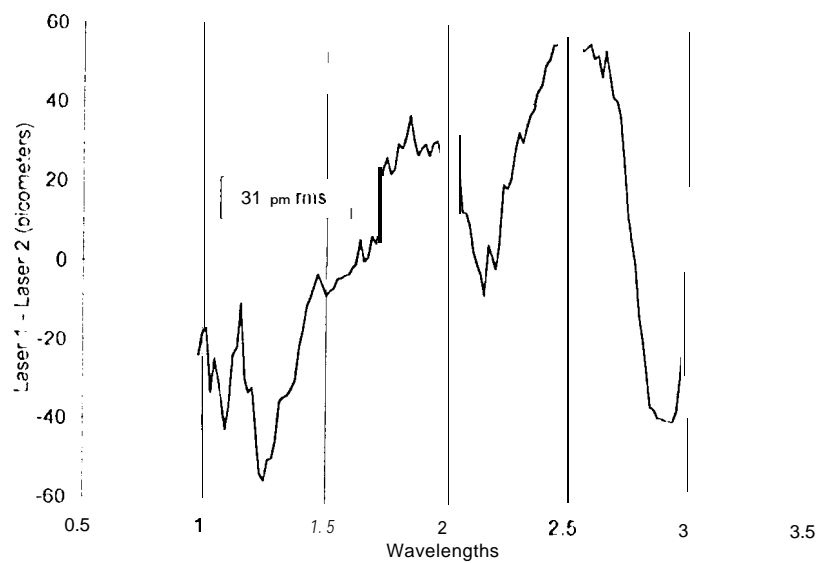
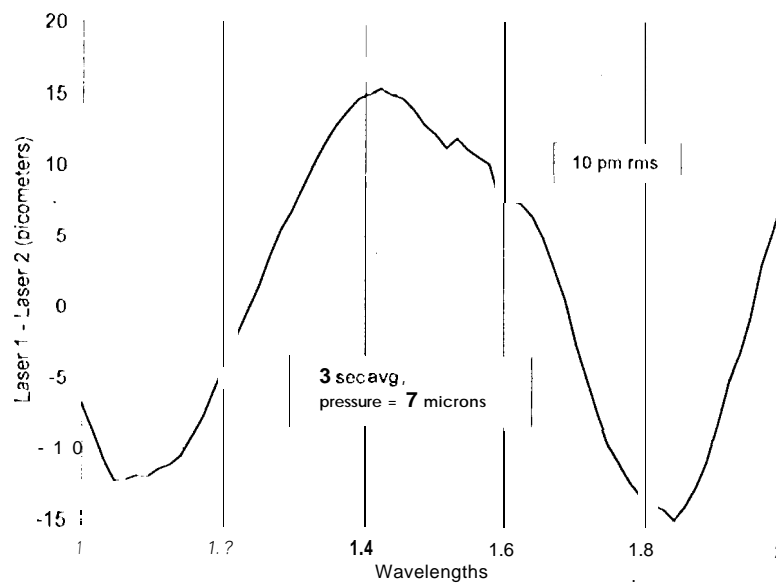


Figure 9: Relative metrology with cyclic averaging in vacuum



To illustrate this, consider the following expression representing the difference between the two interferometer signals with non-linearities and drift:

$$\text{Interf}_1 - \text{Interf}_2 = \sum_{i=0}^N a_i x^i + \sum_{j=0}^M \left(\sum_{k=0}^L b_k x^k \right) \sin(2j\pi x) \quad (1)$$

where a_i and b_k are constants. x is the distance traveled by the corner cube with the piezoelectric transducer. The term $\sum_{i=0}^N a_i x^i$ represents the drift between the two interferometers and the term $\sum_{j=0}^M \left(\sum_{k=0}^L b_k x^k \right) \sin(2j\pi x)$ represents the systematic errors with non-linearities and drifting amplitudes.

A typical term containing the systematic errors is of the form $x^k \sin(2j\pi x)$. Cyclically averaging this gives:

$$\int_q^{q+1} x^k \sin(2j\pi x) dx = - \left(\frac{kq^{k-1} + \text{lower order}}{2j\pi} \right) \cos(2j\pi q) + \frac{k}{2j\pi} \int_q^{q+1} x^{k-1} \cos(2j\pi x) dx \quad (2)$$

Note that cyclically averaging once reduces the exponent x^k from k to $k-1$. Hence, after $k+1$ integrations the term $x^k \sin(2j\pi x)$ will vanish. In general, if the highest power in the self-interference term is L , then $L+1$ cyclic averagings are needed to completely remove self-interference.

The term representing the drift can be recovered after these operations. To illustrate this, let $N=2$ in the drift term. Then,

$$\text{drift} = a_0 + a_1 x + a_2 x^2 \quad (3)$$

After cyclically averaging 1, times:

$$\langle \text{drift} \rangle_L = a_0 + (L/2)a_1 + (1/4)(L-1/3)a_2 + (a_1 + La_2)x + a_2 x^2 \quad (4)$$

Therefore, a_2 can be obtained by a fit; a_1 can be obtained using a_2 and the linear coefficient of the fit; a_0 can be obtained using a_2 , a_1 and the constant term of the fit.

Fig. 10 shows the difference between the two interferometer signals after radiative thermal shields are installed over the experiment in vacuum. Fig. 11 shows the difference after three cyclic averagings and the removal of linear drift. The residual error is 3.5 picometers rms. The linear drift is 33 picometers per wavelength. In this particular experiment, one wavelength was scanned in 2 minutes using 64 steps.

4 ABSOLUTE METROLOGY GAUGE

The OSI absolute metrology gauge is being implemented using a stabilized, solid-state infrared laser driving a heterodyne interferometer monitoring the distance to be measured. The laser frequency is changed by a known amount F and the resulting N fringes are counted by the heterodyne interferometer (Fig. 12). The absolute distance L between the two corner cubes of the heterodyne interferometer is given by $L = cN/F$ where c is the speed of light.

The frequency of the infrared laser has been stabilized to an external Galry-Pot cavity to one part in 10^{10} for time scale of several hours. A small vacuum oven is under construction to stabilize the length of the cavity to the same accuracy for a time scale of 24 hours.

The absolute metrology experiment will be performed by tuning the laser by an amount which is an exact multiple of the longitudinal mode spacing of the cavity. This mode spacing is determined by locking two lasers to the same cavity by one-longitudinal mode apart and by counting the resulting beat frequency.

The infrared laser is capable of tuning over a range of ~ 15 GHz. Our present fringe counter has a fractional counting accuracy 1 part in 5120. These figures indicate that a 10 micron absolute accuracy is achievable with modest improvements.

Figure 10: Relative metrology without cyclic averaging in vacuum

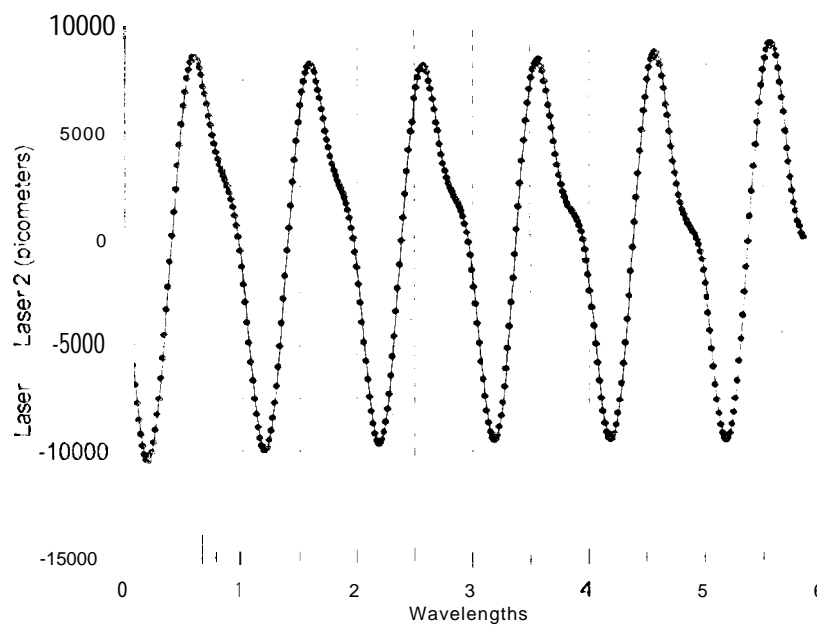


Figure 11: Relative metrology with multiple cyclic averaging in vacuum

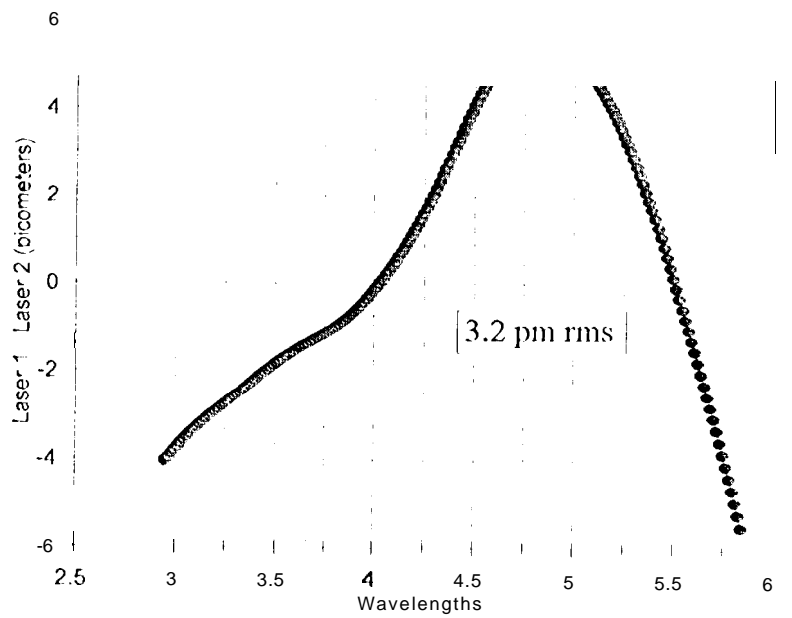
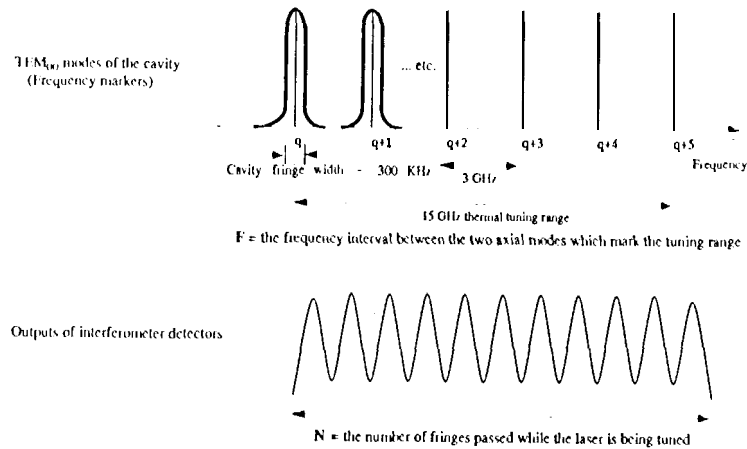


Figure 12: Absolute metrology experiment



Then, the absolute length L is given by:

$$L = c N / F$$

where c is the speed of light

5 C ONCLUSION

The precision and the accuracy of the heterodyne interferometer is improved to picometer level. A faster relative gauge which sweeps the frequency of the laser to implement cyclic averaging is under construction. Feasibility of an absolute metrology gauge using a heterodyne interferometer which has an accuracy of 10 microns over a distance of 10 meters is demonstrated.

G ACKNOWLEDGEMENTS

I would like to thank FvI. Shao, M.M. Colavita, J. Yu and B.E. Hines for many fruitful discussions. The research described was performed at the Jet Propulsion Laboratory, California Institute of Technology, under a contract with the National Aeronautics and Space Administration.

References

- [1] M.D. Rayman, M.M. Colavita, R. N. Mostert, J. Yu, et. al. Orbiting Stellar Interferometer (OSI): FY92 Study Team Progress Report, JPL Publication JPL 1)- 10374, December 14, 1992.
- [2] B. Hines, M. Colavita, K. Wallace, A. Poulsen. SUB-NANOMETER LASER METROLOGY SOME TECHNIQUES AND MODELS, in *Proceedings of the High Resolution Imaging by Interferometry 11*, Garching, Germany, 1991.